HHS Public Access

Author manuscript

Nat Neurosci. Author manuscript; available in PMC 2017 June 05.

Published in final edited form as:

Nat Neurosci. 2017 January ; 20(1): 20–23. doi:10.1038/nn.4452.

Developmentally defined forebrain circuits regulate appetitive and aversive olfactory learning

Nagendran Muthusamy[1,3], **Xuying Zhang**[1,3], **Caroline A. Johnson**[1,3], **Prem N. Yadav**[2], and **H. Troy Ghashghaei**[1,*]

[1]Department of Molecular Biomedical Sciences, College of Veterinary Medicine; North Carolina State University, Raleigh, NC, 27607, USA

[2]Division of Pharmacology, CSIR-Central Drug Research Institute, Lucknow-226031, India

Abstract

Postnatal and adult neurogenesis are region- and modality-specific, but the significance of developmentally distinct neuronal populations remains unclear. We demonstrate that chemogenetic inactivation of a subset of forebrain and olfactory neurons generated at birth disrupts responses to an aversive odor. In contrast, novel appetitive odor learning is sensitive to inactivation of adult born neurons, unveiling that developmentally defined sets of neurons may differentially participate in hedonic aspects of sensory learning.

Keywords

Behavior; Olfaction; Olfactory; Odor; Neurogenesis; Adult; Development; Perinatal; Postnatal; Learning; Learned; Innate; Aversive; Appetitive; subventricular zone; rostral migratory stream; granule; neurons; periglomerular; response; Chemogenetics; DREADDs; Nestin-Cre; Mice

Postnatal neurogenesis occurs in distinct regions of the mammalian central nervous system (CNS) including the hippocampus and the olfactory bulbs (OB). In rodents, neurons generated in the subependymal zone (SEZ) and rostral migratory stream (RMS) move to the OB to integrate into existing circuits as interneurons [1]. Recent findings using toxin-induced cell ablation [2], blockade of SEZ neurogenesis with mitotic inhibitors [3] or irradiation [4] have implicated adult born OB neurons in a range of olfactory functions including odor sensing, odor discrimination, olfactory memory, and social recognition. Olfactory learning has also been linked to enhanced survival of adult born OB neurons [5] and optogenetic activation of these neurons facilitates olfactory memory and performance [6]. However, there are significant challenges associated with non-autonomous effects of toxin-based cell ablation on

*Corresponding author: tghashg@ncsu.edu. Telephone: 919-513-6174. Fax: 919-513-6465. Address: 1060 William Moore Drive, Raleigh, NC 27607, USA.

[3]These authors contributed equally to this work

Contributions: HTG conceived and designed the study. PNY produced AAVs at the initial stages of the project. NM and XZ performed all experiments and collected most data. CAJ collected some data and performed all statistical analyses. NM, XZ, CAJ and HTG analyzed data. NM, CAJ and HTG wrote the manuscript.

Competing Financial Interest: The authors declare no competing financial interest.

surrounding cells and tissues, as well as incomplete and potential off-target effects of anti-mitotic drugs on production of new OB neurons. Moreover, use of optogenetics for selective modulation of OB neurons is difficult due to spatially restricted penetration of light into neuronal tissue in vivo [7], which imposes the requirement for multiple fiber optic implants within OB tissue to control the activity of dispersed neurons. These technical obstacles have limited the ability to directly investigate the behavioral and physiological roles of continuous neuronal integration in the olfactory bulbs [8].

The chemogenetic approach using Designer Receptors Exclusively Activated by Designer Drugs (DREADD) [9] is a far less invasive and an ideal approach for acute control of activity in newborn OB neurons. DREADDs are mutagenized muscarinic acetylcholine receptors that fail to respond to acetylcholine, but can be activated by systemic administration of the physiologically inert small molecule Clozapine N-oxide (CNO), a metabolite of Clozapine. CNO-mediated activation of distinct DREADDs results in depolarization or hyperpolarization of targeted neurons. To selectively express the inhibitory version of DREADDs (Gi) in postnatally born OB neurons, an Adeno associated virus serotype 2 (AAV2) containing Cre-responsive 'FLEX' elements [10] flanking the inverted Gi sequence was injected into the anterior cerebral ventricles of postnatal day 42 (P42) *Nestin-Cre* male mice (Fig. 1a; referred to as 'P42-Gi' herein). To evade expression in stem cells and immature neuroblasts, the vector contained the 'FLEXed' Gi sequence downstream of a human synapsin promoter (*pSYN*; Fig. 1a) [11]. Transduced P42 born OB neurons were tracked four weeks after injection (Supplementary Fig. 1a) using co-expression of an AAV2-*pSYN::EGFP* reporter with either HA-tagged or mCherry-fused Gi (Supplementary Fig. 1b,c). AAV2 mediated expression was largely confined to mature neurons in the OB while absent in SEZ and RMS cells (Supplementary Fig. 1d,e).

The distribution and morphology of $EGFP^+$ neurons in the OB corresponded to cells in the granule cell layer (GCL); some had extensive apical dendrites and others resembled Golgi or star-shaped Blanes cells (Supplementary Fig. 1f) [12]. To test if $EGFP^+$ neurons were active in the OB, mice were administered vehicle or CNO injections and perfused 90 minutes later, followed by staining for c-Fos, a reporter for neuronal activity (Supplementary Fig. 1a). The OBs of CNO-administered P42-Gi mice contained significantly fewer $EGFP^+$/c-Fos^+ double labeled neurons compared to controls (Fig. 1b,c). Thus, selective expression of DREADD-Gi can be targeted to and inhibit a subset of adult-born neurons after CNO administration.

Since newborn OB neurons are responsive to novel odors and are stimulated to form new synapses [13], we tested P42-Gi responses to novel odors. Four weeks after AAV2-Gi administration, CNO- and vehicle-injected mice explored clean test cages for 45 minutes while video recorded (Fig. 2a). Basal behaviors were prevalent in both groups during habituation (Supplementary Fig. 2). Both sets of P42-Gi mice were then tested on ability to find novel appetitive odors buried under the bedding in the test cage (10 minute trials; Treat A: peanut butter cookie, Treat B: mint chocolate cookie). Vehicle-injected mice had a significantly higher number of successful trials than their CNO-administered counterparts over seven days of repeated trials (Fig. 2b). Moreover, the performance of the vehicle group, but not the CNO-injected mice improved during the seven days (Fig. 2c). CNO-administered *Nestin-cre* mice without AAV2-Gi injections performed similar to vehicle-injected P42-Gi

mice (Supplementary Fig. 3a,b,c), ruling out unanticipated effects by CNO. To further test the significance of 'novelty' in responses to appetitive odors, CNO-withheld P42-Gi mice were pre-exposed to either treat in seven daily trials (Supplementary Fig. 3d). This was followed by a second seven-day test trial during which half of the mice received vehicle, and the other half CNO injections. All mice in both groups successfully found the learned treats during the entire period (Supplementary Fig. 3e). Thus, a small subset of P42-born neurons in the OB are critical for successfully retrieving novel, but not learned, appetitive odors.

We next asked if activity of P42-born neurons also plays a role in the expression of fear responses to an aversive odor novel to our mice. To mimic a predator odor we used 2,5-Dihydro-2,4,5-Trimethylthiazoline (TMT), an extract from the red fox anal gland, which is an established mediator of freezing responses in rodents requiring intact olfactory bulbs [14]. P42-Gi mice were exposed to a TMT-treated filter paper placed on one side of a test cage and video recorded for 10 minutes (Fig. 2a). To our surprise, both vehicle- and CNO-injected mice responded to TMT by exhibiting robust freezing (Fig. 2d). Neither the responses during the seven days of repeated exposures (Fig. 2e) nor time spent immobile during the seven days (Fig. 2f) were significantly different from vehicle controls. Similar to the appetitive tests, administration of CNO in *Nestin-cre* mice without intraventricular injections of AAV2-Gi failed to disrupt responses to TMT (Supplementary Fig. 4).

Since heterogeneous populations of neurons begin to integrate into the OB circuitry during perinatal development [15–18], we next asked whether neurons generated soon after birth include a population whose activity is critical for freezing responses to TMT later during early adulthood. P0 *Nestin-Cre* pups were intraventricularly injected with AAV2-Gi (P0-Gi) and allowed to survive to P70 as were P42-Gi mice. Since subventricular stem and progenitor cells were transduced in newborn mice, labeled cells were more abundant and distributed in various forebrain regions outside the OBs compared to P42-Gi mice (Fig. 3a,b). However, the number of counted neurons and their percentages as a fraction of the sampled population transduced in the forebrain was far more in the OB and olfactory related regions (e.g., olfactory nuclei) than in non-olfactory areas (Fig. 3a,b,c; Supplementary Fig. 5). For example, only a miniscule fraction of neurons were found in the amygdala which is known to regulate freezing behaviors (Amy, Fig. 3c). Attempted injections into the olfactory ventricles (OV) to focus AAV2 transduction to OB neurons continued to result in spread to various forebrain regions (Supplementary Fig. 6). At this juncture we presume the spread is due to the open communication between the OV and the lateral ventricles at P0. Despite the larger number of forebrain cells being transduced, CNO- and vehicle- administered P0-Gi mice spent similar proportions of time on exploratory and other basal behaviors when exposed to a novel environment (Supplementary Fig. 7).

Comparison of vehicle- and CNO-injected P0-Gi mice during individual trials of TMT exposure (Fig. 3d) revealed that a higher proportion of the CNO group failed to freeze (Fig. 3e) and responses did not change over the seven test days (Fig. 3f,g). CNO-induced disruption of freezing was independent of fear-associated acoustic startle response (Supplementary. Fig. 8), thus ruling out the potential impact of transduced neurons outside the olfactory circuitries in freezing. Furthermore, performance of P0-Gi mice in the appetitive odor test revealed no significant difference with controls (Fig. 3h,i). These

findings suggest that the freezing response to TMT is most likely associated with olfactory circuitries established perinatally. These forebrain circuitries exhibit little to no involvement in detection and learning of novel appetitive odors and/or related exploratory behaviors.

Since dorsal OB glomeruli are known to participate in eliciting avoidance behaviors in mice in response to aversive odors [14, 19], we next assessed whether AAV2-targeted cells in the P0-Gi OBs were preferentially differentiating in dorsal or ventral glomeruli. Mapping the distribution of $EGFP^+$ neurons in P0-Gi OBs revealed no preference, with substantial distribution in granule, mitral, and glomerular layers of both the ventral and dorsal OB, as well as in the accessory olfactory region (Supplementary Fig. 9). This was in contrast to the largely granule cell layer preference of P42-Gi transduced neurons, where appetitive odor detection could be disrupted by CNO administration. Accordingly, the observed influence of P0-born neurons on detection of the aversive TMT odor is correlated with their differentiation in the periglomerular and mitral cell layers in the OB, in addition to several other olfactory-related nuclei and regions in the forebrain.

Lastly, to examine the proportions of virus-infected cells among newly generated neurons in the OB, Bromodeoxyuridine (BrdU) was administered during the day of AAV2 injections to target progenitors synthesizing DNA at the time of surgery (Supplementary Fig. 10). Only a fraction of $BrdU^+$ cells labeled at P0 or P42 were $EGFP^+$, and likewise only a fraction of $EGFP^+$ cells were $BrdU^+$ by P70. This finding suggests that despite inhibition of only a fraction of developmentally defined cells in the forebrain, activity in their untransduced cohorts is insufficient for mediating detection of new odors. We postulate that developmentally distinct neurons become components of networks wherein small alterations to ensemble activity result in disruption of behavioral outputs. There is precedence for this concept in a recent finding that ensemble activity of central interneurons can be modulated even when only a few neurons within the network are experimentally activated [20]. The precise mechanism of how inactivation of only a fraction of newly integrated cells inhibits a behavior such as finding a novel appetitive odor remains to be determined.

Taken together, our study has unexpectedly exposed two sets of developmentally early- and late-derived neuronal ensembles that independently regulate detection and/or associative learning of novel aversive versus novel appetitive odors. The majority of these neurons differentiate within olfactory associated regions, although we cannot neglect the potential role of neurons targeted by our approach in other forebrain regions. Moreover, since a larger population of neurons were targeted at birth we cannot rule out the possibility that their mere density allows for disruption of detecting aversive odors compared to the lower densities targeted in young adult mice. This finding raises the possibility that unlike attractive odorants, aversive and potentially danger-indicating stimuli may have an innate, and developmentally early, component within the olfactory and related forebrain circuitries. It is tempting to speculate that a hard-wired/innate circuitry established immediately after birth is critical for detection of aversive odorants. This may afford the animal evolutionary or physiological advantage early in life when it must instinctively protect its immediate survival. In contrast, learning new appetitive odors and maintenance of satiety later in life may be necessary for long term survival. The precise specification, identity, and connectome of neuronal circuits regulating hedonic odor detection and learning remain to be elucidated.

Whether or not this theme applies to other sensory and complex behavioral modalities remains to be tested.

Online Methods

Animals

Mice were housed, maintained, and utilized in experiments under the regulations and approval of Institutional Animal Care and Use Committee at North Carolina State University. Male *Nestin-Cre* mice (Tg (Nes-Cre)1KLN/J; Jackson Lab, # 003771) at either day of birth (P0) or postnatal day 42 (P42, six weeks of age) were used in this study. Mice were maintained on a 12 hour light:12 hour dark cycle with access to water and food ad libitum. None of the animals were used in prior experimental procedures unrelated to this study and mice were obtained from independent litters as much as possible.

Viral microinjections

High titer viral stocks of Adeno Associated Virus 2 (AAV2) carrying the constructs pAAV-p*SYN-DIO-EGFP* (6×10^{12} particles/mL) together with pAAV-*pSYN-DIO-HA-hM4D(Gi)-IRES-mCitrine* (2×10^{12} particles/mL) or rAAV2-*pSYN-DIO-hM4D-mcherry* (4×10^{12} particles/mL) were purchased from the Vector Core at University of North Carolina, Chapel Hill. P42 naïve *Nestin-Cre* males were anesthetized using freshly prepared Avertin (375 μg/kg body weight). AAV2 viral stocks (5 μl) were bilaterally injected into the lateral ventricles using a stereotaxic apparatus with coordinates relative to bregma (0.4 mm lateral, 2.5 mm deep). Following injections, mice were allowed to recover under a heat lamp, then placed back in their home cage and allowed to survive to P70, at which time behavioral experiments were performed (referred to as P42-Gi). P0 Nestin-Cre pups were anesthetized by hypothermia and AAV2 viral stocks were injected (2 μl) into the lateral ventricle relative to bregma (0.2 mm lateral, 1.5 mm deep) or olfactory ventricles (0.8 mm anterior, 0.4 mm lateral, 1.5 mm deep). Following injections, pups were recovered under a heat lamp and returned to the nursing dam. P0-Gi mice were weaned normally and subjected to behavioral tasks at P70 (referred to as P0-Gi). Some P0-Gi and P42-Gi mice were intraperitoneally administered BrdU (Sigma; 100 mg/kg body weight; dissolved in saline) once at the end of the surgery for AAV2 injections. Mice were perfused following final testing as described later.

Novel appetitive odor detection task

On each day of behavioral testing, mice were intraperitoneally injected with Clozapine-N-Oxide (CNO; 1mg/kg body weight dissolved in sterile H_2O) twice, with four hours between each injection. Control mice were P0-Gi or P42-Gi mice that only received vehicle injections of sterile H_2O at same volume as would be given with CNO. Additionally, *Nestin-cre* mice without intracerebral AAV2-Gi injections were administered CNO to control for possible effects on behavioral responses. Mice were moved from their home cage to a testing cage immediately following the second CNO or vehicle injections, which was similar to the home cage with fresh bedding, food pellets, water, and equipped with video cameras outside the cage. Mice were allowed to habituate to the testing cage for 45 minutes, after which they were briefly moved to their home cage while the testing cage was prepared for appetitive

novel odor detection task. As a source of novel appetitive odors either peanut butter cookie (Treat A; 1 gram per slice) or mint chocolate cookie (Treat B; 1 gram per slice) was buried approximately two centimeters below the surface of bedding in the testing cage. All mice used for testing were never exposed to either treat prior to testing. Mice were placed in the testing cage, video recorded for 10 minutes and time to finding the treats was quantified post hoc. When mice correctly located and recovered the buried treat it was recorded as a successful trial with the time-to-success measured in the video. Each mouse performed the test once daily for seven consecutive days. Data were plotted and appropriate statistical analyses were performed as indicated.

To test the effects of pre-exposure to treats on novelty task performance, P42-Gi mice were subjected to the task without IP injections for seven consecutive days three weeks after intraventricular injections of AAV2-Gi (beginning at P63). Following pre-exposure, mice were divided into two groups (n=6 each) with one group administered CNO and the other vehicle. Odor detection was video recorded and analyzed in the testing cage as described above.

Novel aversive odor detection task

For testing of responses to an aversive odor, the same behavioral paradigm described above was applied. Fear freezing response was used to measure aversion to an established aversive odor presented by 2 μl of 2,5-Dihydro-2,4,5-trimethylthiazoline (TMT; 1 mg/μl) on a filter paper placed on one side of the testing cage and visible to mice on the bedding. Mice were placed in the testing cage and responses were video recorded and post hoc analyses were performed as described above. Controls were the same as those described for the appetitive odor tests. Freezing behavior was defined as any immobility excluding respiration during the 10 minute test period. Latency to freezing was also measured to assess rate of response to TMT.

Acoustic Startle Test

Mice were acclimated to an SR-LAB Startle Response System (San Diego Instruments) with enclosure centered over a motion sensor for 15 minutes prior to testing without any restraint. The system is coupled to a computer to record the responses of mice. Acclimation was followed by trials without sound stimulus to control for effects of background noise. This was followed by a habituation period during which 10 maximum ‘pulse noise’ stimuli (120 decibels, dB, ~40 ms/pulse) were presented. Mice were then exposed to 84, 88, and 92 dBs of prepulse noises in random order and random intervals. This was followed by presentation of a single startle pulse noise followed by a final train of the same prepulse noises. Responses of mice were recorded by the apparatus in millivolts (mV) and data was transferred to Microsoft Excel for analysis. Responses were averaged over seven days per mouse and presented as a dot plot (Supplementary Fig. 8). Indices of prepulse inhibition were calculated as percentage of pulse test over average responses during the initial trains of pulse noise (% Pulse Noise).

Tissue processing and immunohistochemistry

Mice were intracardially perfused with 4% paraformaldehyde (PFA; in 0.1 M PBS; pH 7.4) 90 minutes after the last testing session, and brains were harvested and post-fixed overnight in 4% PFA at 4°C. Brains were sectioned on a vibratome at 50 μm in the sagittal plane, blocked in 0.1 M PBS containing 10% serum and 1% Triton-X-100 (Sigma) for one hour at room temperature. For staining of BrdU, sections were washed in 2 N HCl for 10 minutes followed by three 5 minute washes in 0.1 M Sodium Borate (pH 8.5), followed by blocking. Sections were incubated with primary antibodies in 0.1 M PBS containing 1% serum and 0.3% Triton-X-100 overnight at 4°C, followed by washing in PBS and incubation with appropriate secondary antibodies for 1–2 hours at room temperature for visualization the next day. Antibodies and stains used: goat anti-cFos (Santa Cruz; 1:1000), chicken anti-GFP (Abcam; 1:2000), rabbit anti-RFP (Abcam; 1:1000), rabbit anti-HA (Cell Signaling; 1:500), mouse anti-NeuN (Millipore; 1:1000), mouse anti-BrdU (Becton Dickinson, 13:1000), guinea pig anti-Dcx (Millipore, 1:1000), and DAPI (nuclear stain; Sigma; 1:2000). Labeled sections were imaged on Fluoview 1000 (Olympus) or C1 (Nikon) confocal microscopes and double labeling was confirmed by z-stack analyses in the IMARIS software.

Cell counting and analyses

Percentages of double labeled cells were calculated from 60x (Olympus oil lens) confocal image stacks, 0.5 μm intervals in the z-plane and 1024 × 1024 resolution in the xy-plane (0.24 μm per pixel). Images were obtained from sagittal sections of P42-Gi or P0-Gi brains that were perfused 90 minutes after CNO or vehicle injections. Counting frames (210 μm × 210 μm) were captured from random areas in the olfactory bulbs, and were analyzed in Image J using the Cell Counter plugin (ImageJ, US National Institutes of Health). Colocalization was confirmed in z-stacks of confocal images. For analysis of c-Fos colocalization with EGFP, all cells within multiple frames were counted until a total of 300 EGFP+ was reached within each animal. For analysis of overlap of AAV2 transduced cells (EGFP+) with HA- or mCherry-tagged Gi (Supplementary Fig. 1), and BrdU (Supplementary Fig. 10) all cells within multiple frames were counted until a total of 100 EGFP+ was reached within each animal. Data were transferred to Microsoft Excel for statistical analyses.

Number of $EGFP^+$ cells in various nuclear and cortical forebrain structures in P0-Gi and P42-Gi mice were counted in tile-scanned confocal images of sagittal sections from three mice in each group (18 sections containing $EGFP^+$ cells in areas and nuclei identified in pilot studies, 20x objective, 1024 × 1024 resolution, 0.62 μm per pixel). DAPI counterstain was used to delineate architectonic boundaries using the Allen Brain Atlas P56 mouse sagittal reference panels (http://atlas.brain-map.org/atlas?atlas=2).

Statistics

Data collection and analyses were not performed blind to the conditions of the experiments. No data points were removed from statistical analyses. Sample sizes for behavioral experiments were not determined statistically but are in accordance with common practice [1, 2]. All statistical analyses were conducted in Microsoft Excel and GraphPad Prism. Data are presented in dot plots with lines indicating mean ± s.e.m., and interquartile ranges

are available when appropriate in the supplementary methods checklist. Temporal dot plots show individual values for each mouse over seven days of testing. Trendlines were obtained using Graphpad Prism generate linear regressions and associated 95 percent confidence intervals of proportions of failed trials or average time spent immobile over time for each group.

For cellular data, two-tailed unpaired t-test was employed for comparison of percentages of cell numbers between groups (normality was assumed but not formally tested). Cellular data was collected from randomly selected regions and sections. Behavioral data could not be tested for normality due to small sample size, therefore nonparametric statistics was employed. Assignment of mice to vehicle or CNO groups was arbitrary but not formally randomized. Two-tailed Mann Whitney U test was used when comparing time spent in behaviors or acoustic startle response between groups. Fisher's Exact Test was used when comparing binary trial outcomes (success/failure; freeze/no freeze) between groups. Hypothesis testing of linear regression slopes was used to determine if the rate of change in binary outcomes and time spent immobile was different between groups. Significance was defined as $P<0.05$.

Data availability

Data that support the findings of this study are available from the corresponding author upon request.

Supplementary Material

Refer to Web version on PubMed Central for supplementary material.

Acknowledgments

We thank Drs. David Dorman and Melanie Foster for sharing their Startle Response System, and Bryan Roth for discussions at the onset of the study. HTG is supported by grants from the National Institutes of Health (R01NS098370 and R01NS089795).

References

1. Lim DA, Alvarez-Buylla A. Adult neural stem cells stake their ground. Trends Neurosci. 2014; 37:563–571. [PubMed: 25223700]
2. Sakamoto M, et al. Continuous neurogenesis in the adult forebrain is required for innate olfactory responses. Proc Natl Acad Sci U SA. 2011; 108:8479–8484.
3. Mak GK, et al. Male pheromone-stimulated neurogenesis in the adult female brain: possible role in mating behavior. Nat Neurosci. 2007; 10:1003–1011. [PubMed: 17603480]
4. Feierstein CE, et al. Disruption of Adult Neurogenesis in the Olfactory Bulb Affects Social Interaction but not Maternal Behavior. Front Behav Neurosci. 2010; 4:176. [PubMed: 21160552]
5. Sultan S, et al. Learning-dependent neurogenesis in the olfactory bulb determines long-term olfactory memory. FASEB J. 2010; 24:2355–2363. [PubMed: 20215526]
6. Alonso M, et al. Activation of adult-born neurons facilitates learning and memory. Nat Neurosci. 2012; 15:897–904. [PubMed: 22581183]
7. Yizhar O, Fenno LE, Davidson TJ, Mogri M, Deisseroth K. Optogenetics in neural systems. Neuron. 2011; 71:9–34. [PubMed: 21745635]
8. Sakamoto M, Kageyama R, Imayoshi I. The functional significance of newly born neurons integrated into olfactory bulb circuits. Front Neurosci. 2014; 8:121. [PubMed: 24904263]

9. Urban DJ, Roth BL. DREADDs (designer receptors exclusively activated by designer drugs): chemogenetic tools with therapeutic utility. Annu Rev Pharmacol Toxicol. 2015; 55:399–417. [PubMed: 25292433]
10. Schnutgen F, et al. A directional strategy for monitoring Cre-mediated recombination at the cellular level in the mouse. Nat Biotechnol. 2003; 21:562–565. [PubMed: 12665802]
11. Kugler S, Lingor P, Scholl U, Zolotukhin S, Bahr M. Differential transgene expression in brain cells in vivo and in vitro from AAV-2 vectors with small transcriptional control units. Virology. 2003; 311:89–95. [PubMed: 12832206]
12. Pressler RT, Rozman PA, Strowbridge BW. Voltage-dependent intrinsic bursting in olfactory bulb Golgi cells. Learn Mem. 2013; 20:459–466. [PubMed: 23950193]
13. Magavi SS, Mitchell BD, Szentirmai O, Carter BS, Macklis JD. Adult-born and preexisting olfactory granule neurons undergo distinct experience-dependent modifications of their olfactory responses in vivo. J Neurosci. 2005; 25:10729–10739. [PubMed: 16291946]
14. Kobayakawa K, et al. Innate versus learned odour processing in the mouse olfactory bulb. Nature. 2007; 450:503–508. [PubMed: 17989651]
15. Garcia I, et al. Local corticotropin releasing hormone (CRH) signals to its receptor CRHR1 during postnatal development of the mouse olfactory bulb. Brain Struct Funct. 2014
16. Sakamoto M, et al. Continuous postnatal neurogenesis contributes to formation of the olfactory bulb neural circuits and flexible olfactory associative learning. J Neurosci. 2014; 34:5788–5799. [PubMed: 24760839]
17. Jacquet BV, et al. Specification of a Foxj1-Dependent Lineage in the Forebrain Is Required for Embryonic-to-Postnatal Transition of Neurogenesis in the Olfactory Bulb. J Neurosci. 2011; 31:9368–9382. [PubMed: 21697387]
18. Lledo PM, Merkle FT, Alvarez-Buylla A. Origin and function of olfactory bulb interneuron diversity. Trends Neurosci. 2008
19. Dewan A, Pacifico R, Zhan R, Rinberg D, Bozza T. Non-redundant coding of aversive odours in the main olfactory pathway. Nature. 2013; 497:486–489. [PubMed: 23624375]
20. Karnani MM, et al. Cooperative Subnetworks of Molecularly Similar Interneurons in Mouse Neocortex. Neuron. 2016; 90:86–100. [PubMed: 27021171]

References

1. Nehrenberg DL, Sheikh A, Ghashghaei HT. Identification of neuronal loci involved with displays of affective aggression in NC900 mice. Brain Struct Funct. 2013; 218:1033–1049. [PubMed: 22847115]
2. Hammad M, et al. Transplantation of GABAergic Interneurons into the Neonatal Primary Visual Cortex Reduces Absence Seizures in Stargazer Mice. Cereb Cortex. 2014; 25:2970–2979. [PubMed: 24812085]

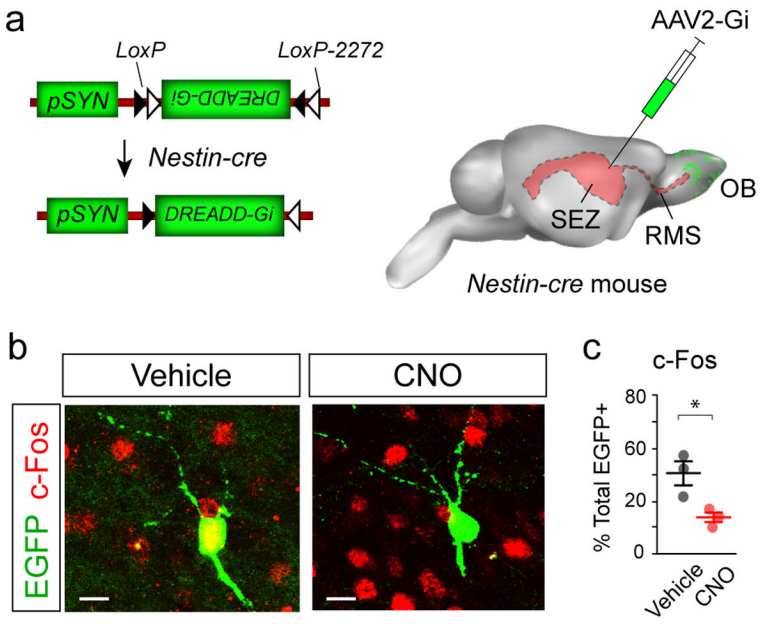

Figure 1. Targeting DREADDs to adult-born neurons in the OB

(a) AAV2 vectors encoding cre-responsive DREADD-Gi and EGFP downstream of the human Synapsin promoter (*pSYN*; AAV2-Gi) were injected into the lateral ventricles of P42 *Nestin-cre* mice to target endogenous neural stem cells (P42-Gi mice). **(b)** Examples of $EGFP^+$ cells in the P42-Gi OB at P70, and their colocalization with c-Fos after vehicle or CNO administration. Scale bars, 10 μm. **(c)** Dot plot of $EGFP^+$/$c\text{-}Fos^+$ double-labeled OB neurons calculated as percentages of total EGFP cells counted in vehicle- and CNO-administered P42-Gi mice. Significance ($P<0.05$, *) was tested by *unpaired t test*, percent double labeled, vehicle: 42.2% ± 5.5%, CNO: 20.1% ± 2.1%; $t(4) = 3.72$, $P = 0.02$.; n=100 EGFP+ cells/mouse, 3 mice/group. Data are mean ± s.e.m.

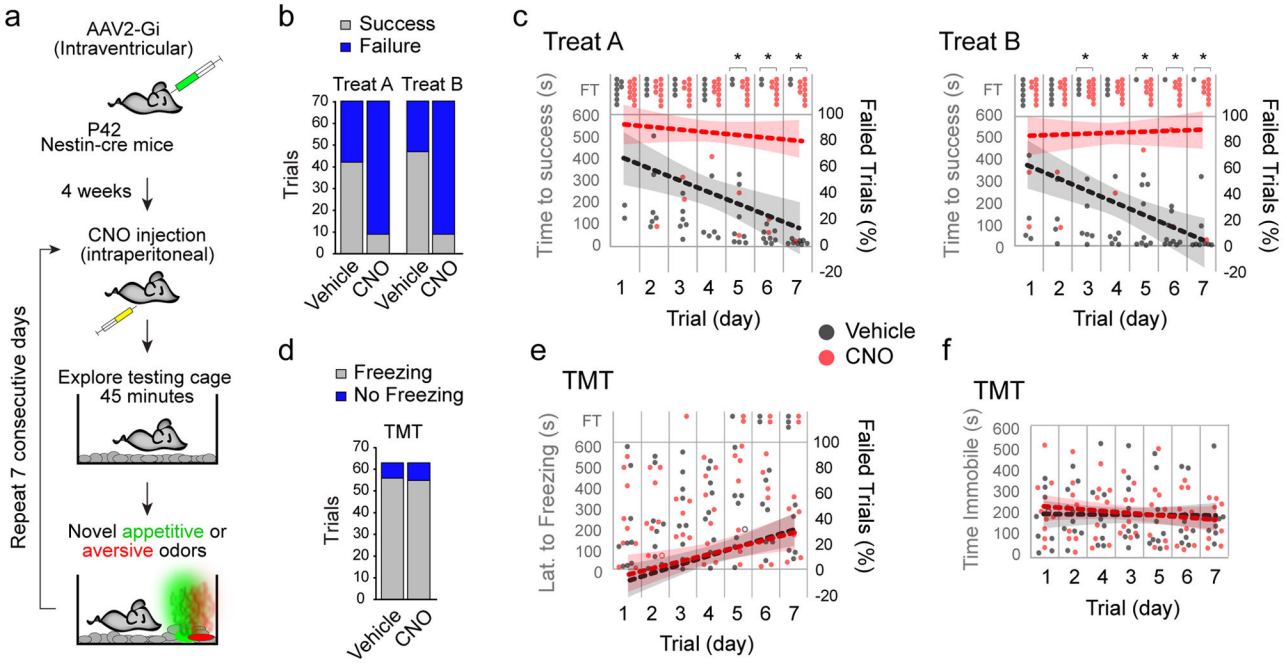

Figure 2. Inhibition of young adult born neurons disrupts responses to novel appetitive, but not aversive odors

(a) Flowchart of strategy to inhibit new neurons in the OB in P42-Gi in the presence of novel appetitive (Treats A and B, green) or aversive (TMT; red) odors over seven consecutive test days. **(b)** Proportions of successful and failed trials in P42-Gi mice administered vehicle or CNO over seven days. Significance was determined by *Fisher's Exact Test* (Number of successful trials, Treat A: vehicle, 42/70; CNO, 9/70; $P=7.6\times10^{-9}$; Treat B: vehicle, 47/70; CNO, 9/70; $P = 4.4\times10^{-11}$; n=10 mice/group). **(c)** Temporal plot of time to finding Treats A and B by all vehicle and CNO treated P42-Gi mice within the 10 minute test period (y-axis) over the seven days (x-axis). FT, failed trial. Dotted lines represent trendlines calculated from proportions of failed trials (right y-axis) over seven days (shaded regions = 95% confidence intervals, CI). Significance was determined by *hypothesis test of linear regression* of proportions of failed trials over seven days [slopes (vehicle): Treat A= −8.9% ± 2.8%/day, CI: −14.45, −3.4; Treat B= −10.0% ± 1.6%/day, CI: −15.15, −4.85. slopes (CNO): Treat A= −1.79% ± 2.0%/day, CI: −5.82, 2.25; Treat B= 0.7% ± 1.5%/day, CI: −3.34, 4.76; H_0: slope (vehicle) = slope (CNO); Treat A, F(1,136)=4.35, P=0.039; Treat B, F(1,136), P=0.0014; n=10 mice/group]. *Fisher's Exact Test* was used to compare proportions of successful trials each day (Treat A, days 1 to 7 in order: P= 0.47, 0.14, 0.17, 0.35, 0.023, 0.023, 0.005; Treat B: days 1 to 7 in order: P=0.63, 0.63, 0.011, 0.057, 0.001, 0.006, 0.001; n=10 mice/group; *, P<0.05). **(d)** Bar chart illustrates proportions of freezing trials in response to TMT in P42-Gi mice administered vehicle or CNO over seven days. Significance determined by *Fisher's Exact Test* (Number of trials freezing: vehicle, 56/63; CNO, 55/63; P=0.99; n=9 mice/group). **(e)** Temporal plot of responses to TMT by all vehicle and CNO treated P42-Gi mice within the 10 minute test period as in (c). Significance was determined by *hypothesis test of linear regression* of proportions of freezing trials over seven days (slope (vehicle): 6.75% ± 1.82%, CI: 3.11, 10.38; slope (CNO): 5.56% ± 2.1%, CI: 1.54, 9.57; H_0: slope (vehicle) = slope (CNO); F(1,122)=0.19, P=0.66). *Fisher's Exact*

Test was used to compare proportions of Freezing trials each day (days 1 to 7 in order: P= 1.0, 1.0, 1.0, 1.0, 1.0, 1.0, 1.0; n=9 mice/group). **(f)** Temporal plot of time spent immobile by vehicle and CNO treated P42-Gi mice within the 10 minute test period (y-axis) over the seven days (x-axis). Significance was determined by *Mann-Whitney U test* (mean ± s.e.m: vehicle, 193.3 ± 5.3 s.; CNO, 203.3 ± 7.2 s.; P=0.26, U=15.0) hypothesis test of linear regression [slope (vehicle): −1.36 ± 8.55 seconds/day, CI: −18.44, 15.73: slope (CNO): −8.10 ± 8.0 seconds/day, CI: −24.12, 7.88; H_0: slope (vehicle) = slope (CNO); F(1,122)=0.33, P=0.56].

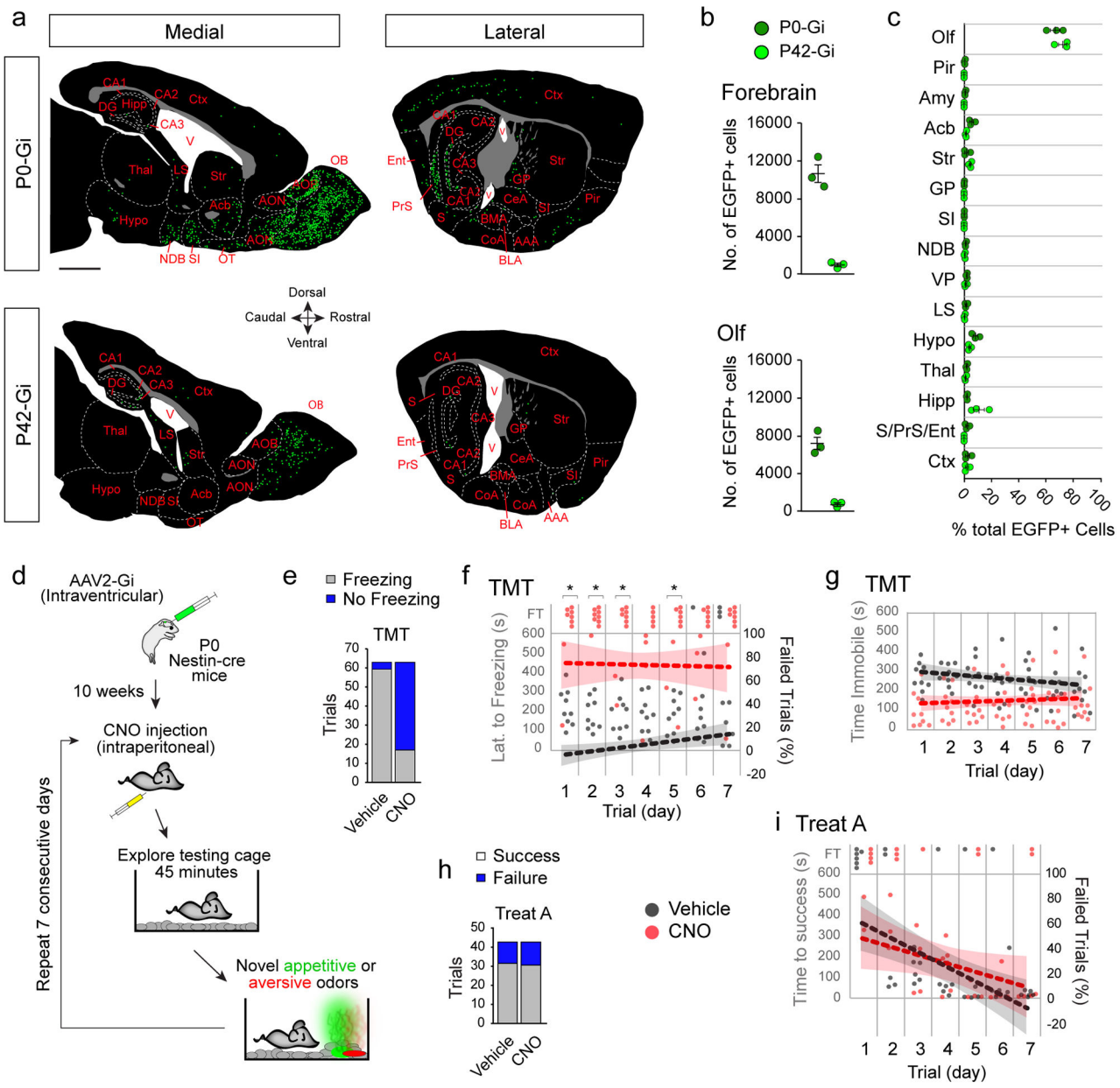

Figure 3. Inhibition of perinatally born neurons disrupts responses to novel aversive but not novel appetitive odors

(a) Tracings of representative medial and lateral sagittal forebrain sections of P0-Gi and P42-Gi mice with areal and nuclear boundaries demarcated by dashed lines. Green dots represent 1–3 EGFP^{+} neurons found in the sections. Scale bar, 1 mm. Abbreviations: ***Olfactory related areas and nuclei (Olf):*** olfactory bulb (OB), anterior olfactory nuclei (AON), accessory olfactory bulb (AOB), olfactory tubercle (OT), Piriform cortex (Pir); ***Amygdalar nuclei (Amy):*** cortical amygdala (CoA), basolateral nucleus (BLA), basomedial nucleus (BM), central nucleus (CeL), anterior amygdalar area (AAA); ***Hippocampus (Hipp) and related areas:*** Cornu Ammonis (CA1, CA2, CA3), dentate gyrus (DG), subiculum (S), presubiculum (PrS), entorhinal cortex (Ent); ***Other nuclei:*** nucleus Accumbens (Acb),

diagonal band nucleus (NDB), ventral pallidum (VP), lateral septal nucleus (LS), Hypothalamus (Hypo), Thalamus (Thal), cerebral cortices (Ctx), Striatum (St), globus pallidus (GP), Substantia Innominata (SI). **(b)** Number of neurons counted in P0-Gi and P42-Gi forebrains and olfactory regions (Olf; mean ± s.e.m. n=3 mice/group). **(c)** Percentages of total number of $EGFP^+$ neurons in various forebrain regions (n=3 mice/group). **(d)** Strategy to inhibit perinatally born neurons in P0-Gi mice and testing over seven days with appetitive and aversive odors beginning at P70. **(e)** Proportions of freezing trials in response to TMT in P0-Gi mice injected with vehicle or CNO over seven days. Significance was tested by *Fisher's Exact Test* (Number of trials freezing: vehicle, 59/63; CNO, 17/63; $P=2.99\times10^{-15}$; n=9 mice/group). **(f)** Temporal plot of responses to TMT by all vehicle- and CNO-treated P0-Gi mice within the 10 minute test period (y-axis) over the seven days (x-axis). FT, failed trials. Dotted lines represent trendlines calculated from proportions of failed trials (right y-axis) over seven days (shaded regions represent 95% confidence intervals, CI). Significance was determined by *hypothesis test of linear regression* of proportions of failed trials over seven days [slope (vehicle): 3.18% ± 1.3%/day, CI: 0.57, 5.78; slope (CNO): −0.4% ± 2.84%/day, CI: −6.08, 5.29; H_0: slope (vehicle) = slope (CNO); F(1,122)=1.31, P=0.26]. *Fisher's Exact Test* was used to compare proportions of Freezing trials each day (days 1 to 7 in order: P= 0.005, 0.005, 0.005, 0.06, 0.02, 0.02, 0.17; *, P<0.05). **(g)** Temporal plot of time spent immobile by vehicle- and CNO-treated P0-Gi mice within the 10 minute test period as in (f). Significance was tested for time spent immobile per day (*Mann-Whitney U test*; mean ± s.e.m: vehicle, 252.6 ± 9.5 seconds; CNO, 144.4 ± 5.8 seconds; P=0.0006, U=0), and *hypothesis test of linear regression* [slope (vehicle): −10.64 ± 5.78 seconds/day, CI: −22.2, 0.92; slope (CNO): 3.66 ± 5.4 seconds/day, CI: −7.08, 14.39; H_0: slope (vehicle) = slope (CNO); F(1,122)=3.28, P=0.07). **(h)** Proportions of successful and failed trials in finding appetitive Treat A by vehicle- or CNO-administered P0-Gi mice over seven days (*Fisher's Exact Test*; Number of successful trials, vehicle, 31/42; CNO, 30/42; P=0.99; n=6 mice/group). **(i)** Temporal plot of responses to Treat A by all vehicle- and CNO-treated P0-Gi mice within the 10 minute test period (left y-axis) over the seven days (x-axis). FT, failed trial. Dotted lines represent trendlines calculated from proportions of failed trials (right y-axis) over seven days. Significance was tested by *Hypothesis test of Linear Regression* [Slope (vehicle): −11.31% ± 2.98%/day, CI: −17.33, −5.29; slope (CNO): −6.55% ± 3.42%/day, CI: −13.46, 0.36; H_0: slope (vehicle) = slope (CNO); F(1,80)=1.10, P=0.30]. *Fisher's Exact Test* was used to compare proportions of successful trials each day (days 1 to 7 in order: P= 0.45, 1.0, 1.0, 1.0, 1.0, 0.45).